RELATÓRIO CIENTÍFICO

Caracterização pan-câncer da intercomunicação de células únicas do microambiente tumoral

(CAPES-PRINT #88887.891948/2023-00)

Período de Vigência do Projeto: novembro/2023 a junho/2024

Pós-doutoranda: Dra. Sarah Santiloni Cury

Supervisor: Dr. Robson Francisco Carvalho
Prof. Assistente Doutor - Departamento de Biologia Estrutural e Funcional – IBB/UNESP, Brasil

Programa de Pós-Graduação:
Ciências Biológicas (Genética)

Instituição:
Instituto de Biociências de Botucatu– IBB
Universidade Estadual Paulista "Júlio de Mesquita Filho" - UNESP

Botucatu 2024

Resumo

O microambiente tumoral (MAT) facilita as interações celulares no câncer através de contato direto ou por fatores secretados (secretoma). Evidências destacam o papel central das células do MAT na secreção de fatores que modulam a infiltração e a função das células tumorais. A caquexia do câncer exemplifica as repercussões dessa interação complexa dentro do MAT. Esta síndrome complexa, marcada por declínio funcional e mortalidade, é desencadeada. Principalmente, for fatores do secretoma do MAT. No entanto, nenhum estudo foi conduzido para caracterizar o repertório global do secretoma das células individuais do MAT e seu perfil de interação induzido usando sequenciamento de RNA de célula única (scRNA-Seq) em vários tipos de tumor com prevalência variável de caquexia. Reanalisamos os dados de scRNA-Seq no banco de dados *Cancer Curated Cell Atlas* (3CA). Usando o pacote Seurat v.4.0.6, caracterizamos os perfis de expressão gênica do secretoma em 12 tipos de tumor. Isso envolveu a análise de cada população de células dentro do MAT, somando 245 amostras tumorais e 829.984 células únicas. Os genes de cada tipo celular foram filtrados usando a lista de genes do secretoma humano do banco de dados *The Human Protein Atlas*. Identificamos também interações cruciais secretoma-receptor correlacionadas com a caquexia do câncer usando o CellChat v.1.6.0. Selecionamos células malignas, células T, células B, macrófagos, fibroblastos, células dendríticas e células endoteliais para análise, considerando que foram encontradas na maioria dos tipos de câncer (> 8 tipos). Análises de comunicação célula-célula baseadas no secretoma demonstraram que a alta prevalência de caquexia se correlaciona com interações aumentadas promovidas por fibroblastos, macrófagos e células malignas. Essas interações também indicam o papel essencial do secretoma dos fibroblastos em cânceres com alta prevalência de caquexia, com o câncer pancreático, impactando o maior número de vias de comunicação célula-célula. Entre as probabilidades de interação, *MDK* expresso por fibroblastos e seu receptor *SDC4*, expressos por células malignas, correlacionam-se positivamente (0,89; p=0,003) com a prevalência de caquexia. Nosso estudo fornece uma abordagem pan-câncer para entender comunicações celulares promovidas pelo secretoma tumoral na caquexia associada ao câncer a nível de célula única. Ao caracterizar perfis de expressão específicos de célula e interações ligante-receptor cruciais, identificamos os fibroblastos como principal mediador, particularmente no câncer pancreático. Esses resultados podem guiar o desenvolvimento de terapias mais direcionadas para as interações relevantes no MAT de tipos de câncer altamente associados à síndrome.

Atividades Realizadas no Período Referente ao Presente Relatório

No período anterior e referente ao presente relatório (novembro/2023 a junho/2024), foram realizadas as seguintes atividades:

1. Seleção dos conjuntos de dados de scRNA-Seq;
2. Análise de scRNA-Seq pan-câncer (12 tipos tumorais e ~1 milhão de células);
3. Análise de perfil do secretoma pan-câncer de sete tipos celulares;
4. Identificação de comunicação intercelular usando CellChat;
5. Análise de correlação de Pearson entre escores de comunicação e prevalência de caquexia;
6. Preparo do manuscrito a ser submetido em revista científica internacional.

1. Justificativa do Projeto de Pesquisa

A caquexia é uma síndrome caracterizada pela perda progressiva de peso que leva a menor resposta ao tratamento e sobrevida de pacientes com câncer. Cânceres do trato gastrointestinal possuem alta prevalência de caquexia, enquanto mama e próstata apresentam menores taxas. O microambiente tumoral (MAT) é composto por componentes celulares e acelulares que promovem a intercomunicação celular. Essas comunicações ocorrem por interações moleculares, que levam ao contato direto célula-célula ou partir de ligantes que interagem com receptores de membrana de outras células do MAT ou moléculas da matriz extracelular. A interação entre células do MAT é associada com iniciação tumoral, metástases e resposta ao tratamento. Por isso, a intercomunicação no MAT pode estar associada à caquexia. Estudo pan-câncer com dados de single-cell RNA-Seq (scRNA-seq) revelou que o estado funcional da célula induz alterações no MAT, por exemplo, células malignas que expressam genes relacionados à resposta por interferon possuem proximidade espacial com células T e macrófagos, enquanto células B aproximam-se de células neoplásicas com aumento do ciclo celular. Entretanto, ainda é necessário investigar as intercomunicações através de sinalizações celulares e redes de interação entre as células normais e malignas do MAT nos tipos tumorais com diferentes prevalências de caquexia

2. Objetivo

Avaliar as intercomunicações celulares entre as células normais e malignas do MAT em tipos tumorais com diferentes prevalências de caquexia

3. Detalhamento das Atividades Referentes ao Projeto de Pesquisa

O detalhamento será subdividido em metodologia, resultados e considerações finais. Para facilitar posterior submissão em revista da área, essa sessão será apresentada em inglês e formato de manuscrito científico.

Methods

Data acquisition and single-cell RNA sequencing (scRNA-seq) data analysis

We reanalyzed public scRNA-seq data to determine the transcriptional profile of secretome genes. We downloaded scRNA-seq data from Curated Cancer Cell Atlas (3CA;

https://www.weizmann.ac.il/sites/3CA/)[1] of the following cancer types: Breast (GSE148673, GSE161529, and E-MTAB-8107), brain (EGAS00001002185, EGAS00001001900, and EGAS00001003845), colorectal (EGAS00001003779), head and neck (GSE150430), hematologic (PRJNA694128), kidney (EGAS00001002325, GSE159115, phs002065.v1.p1, nc9bc8dn4m.1), lung (GSE131907, GSE123904, HRA000154, and E-MTAB-6149), neuroendocrine (EGAS00001004388, EGAD00001008345, GSE137804), ovarian (E-MTAB-8107), pancreatic (GSE154778, CRA001160, GSE155698), prostate (GSE141445), and skin cancer. These cancer types were selected based on our inclusion criteria, which were datasets with primary and untreated samples belonging to the 10X platform (**Supplementary Table 1**). The count data were processed using the Seurat[2] v4.0.6 package in RStudio software. We performed integration across datasets from the same cancer type using *IntegrateData* from Seurat[3]. The identities of cell types were manually annotated based on the expression of canonical markers, we also used the 3CA provided cell type annotations which we utilized to cross-check the de novo cell type annotations. The malignant cells were classified according to the copy number alteration (CNA) inference, reported in 3CA.

Secretome prediction and characterization in cancer single-cells

The DEGs from each cell type were filtered using the list of human secretome from The Human Protein Atlas (https://www.proteinatlas.org/; 1903 secretome genes). The average expression values were selected for visual representation and clusterization in the ggplot2 to generate Principal Component Analysis (PCA).

CellChat to infer cell-cell communication in tumor microenvironment (TME)

We quantitatively inferred and analyzed cellular communication networks induced by the secretome from the scRNA-seq data using CellChat (v.1.6.0)[4]. To identify the potential ligand-receptor interactions between the cell types identified in TME in each cancer type, we loaded the Seurat object into CellChat (https://github.com/sqjin/CellChat/; accessed on 11/04/2023) using the default parameters. This analysis included ~2021 human-validated interactions for secreted signaling and extracellular matrix receptor interactions.

Correlation analyses

We calculated the cachexia prevalence from the Poisson et al.[5] analysis. For neuroendocrine tumors we sourced cachexia prevalence data from Brinksma et al.[6]. Furthermore, we incorporated cachexia prevalence and weight loss data previously described in Freire et al.[7]. Pearson correlation analysis was performed using GraphPad Prism® (GraphPad Software, v5.0, 2008 USA) using communication scores predicted by CellChat and cachexia prevalence (%) in human cancers.

Results

Identification of common cell types in various cancer types and secretome characterization in pan-cancer

Initially, we started our analysis investigating 14 cancer types available on 3CA. However, scRNA-seq data were obtained from 265 tumor samples and 829,984 single cells comprising 12 cancer types from 3CA that met our inclusion criteria. These tumors were selected to allow a comparison between cancer types ranging from high to low prevalence of cachexia. To compare the secretome profile of the same cell type across different tumor types, we first selected the tumor types presenting commonly found cell types. For this reason, we excluded the brain and myeloma from the secretome prediction and communication analysis. Overall, we selected the Malignant, T cell, B cell, Macrophages, Fibroblasts, Dendritic cell (DC), and Endothelial cell types for further analysis because these cells were found in at least 8 out of 10 cancer types (**Figure 1A**). The percentage of these cell types was not correlated with cachexia prevalence, however, we found a trend in correlation among the highly cachectic tumors, such as pancreatic, colorectal, lung, and head and neck cancers (**Figure 1B**). For the immune fraction (macrophage, T cell, B cell, and DC combined) we found a negative correlation, while for the stromal-vascular fraction (fibroblast and endothelial cells combined) we found positive correlations with cachexia prevalence (**Figure 1B**).

Applying PCA to the gene expression data of 1022 secretome genes, we observed a clustering of cell types independent of tumor type (**Figure 1C**). This finding underscores the cell type-specific nature of the cancer secretome, which remains consistent across different cancer types.

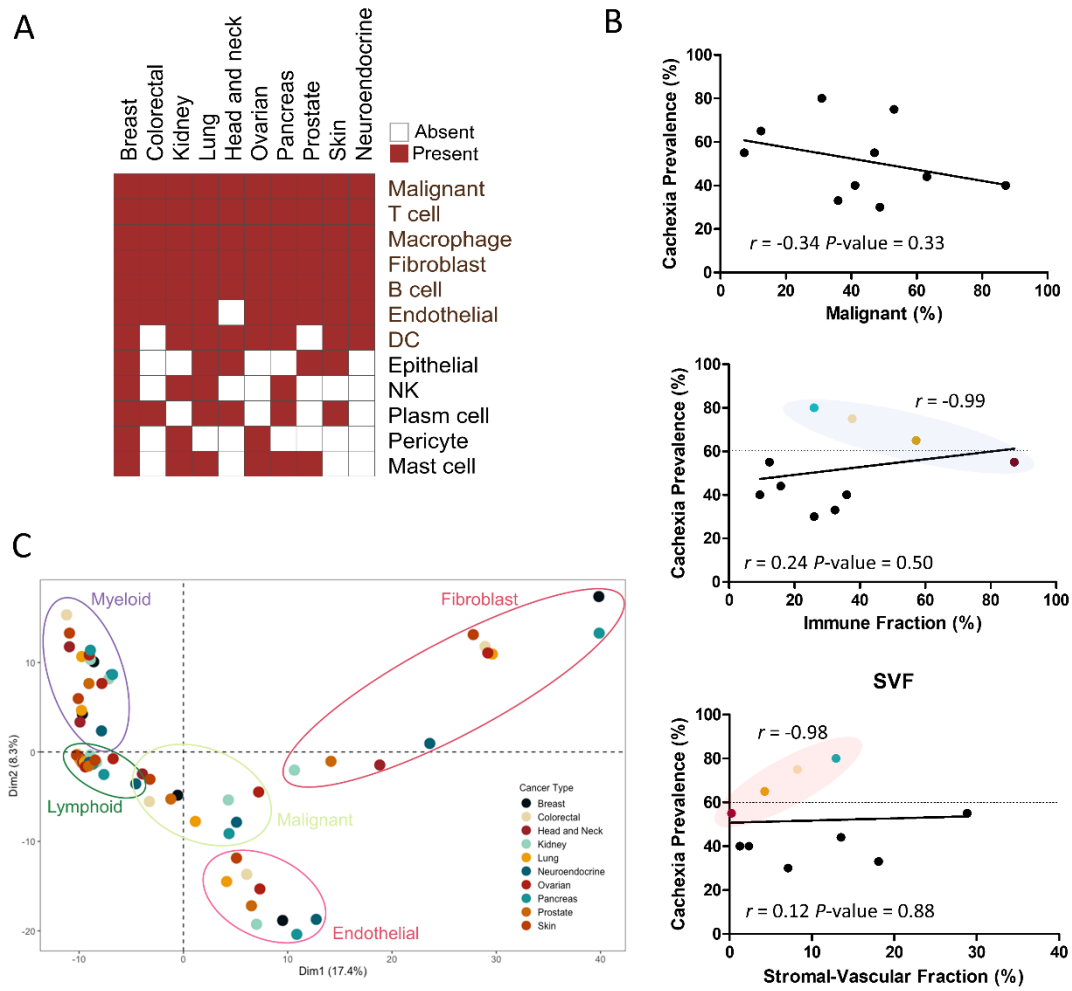

Figure 1. The comprehensive expression profile of the cell type composition and secretome in human cancer single cells. A) Heatmap showing the presence of different cell types in human cancers. **B)** Scatterplot showing the Pearson correlation of the proportion of malignant, immune fraction (T cell, B cell, macrophage, and dendritic cells - DC) and stromal-vascular fraction (SVF; fibroblasts and endothelial) cells with cachexia prevalence. **C)** Principal component analysis (PCA) of the secretome gene expression data in seven cell types among 10 cancer types.

Comprehensive analysis of the ligand and receptor interactions in the tumor microenvironment.

We next asked whether the secretome was promoting different patterns of cell-cell communication within the TME cell in the human cancer evaluated. We first found that the number of interactions increases with the increase of cachexia prevalence in malignant, macrophage, and fibroblasts (**Figure 2A**). By analyzing the pathways that are altered by the cell-cell communications induced by the secretome, we identified that pancreatic cancer has a higher number of pathways (N = 41 communication pathways) involved in cell interactions mediated by the secretome when compared to other cancer types not associated with high cachexia prevalence, such as breast cancer (N = 19 communication pathways). Moreover, the relative information flow was higher in

pancreatic cancer, specially in insulin, CD40, and TGFβ associated pathways (**Figure 2B**). This suggests that pancreatic cancer is not just highly secretory but also highly communicative compared to other types of cancer. We next investigated the cell types that were contributing to this intercommunication, we found that stroma cells (fibroblasts and endothelial cells; sender) communicate with malignant cells (receiver) with higher strength (**Figure 2C**). Considering the relevance of fibroblasts in our findings, we next explored genes that facilitate interactions between fibroblasts and malignant cells, which correlate with cachexia prevalence. Notably, our findings unveiled syndecan-4 (*SDC4*) as the receptor gene within malignant cells that interacts with multiple secretome genes released by fibroblasts (**Figure 2D**). We found *MDK*, secreted by fibroblast, strongly interacting with *SDC4* in malignant cells. The probability of this interaction demonstrated the highest correlation ($r = 0.89$) with cachexia prevalence in cancers (**Figure 2E**). Our results suggest that the increased TME cell-cell communications are associated with cachexia, especially the ones induced by malignant, macrophages, and fibroblasts.

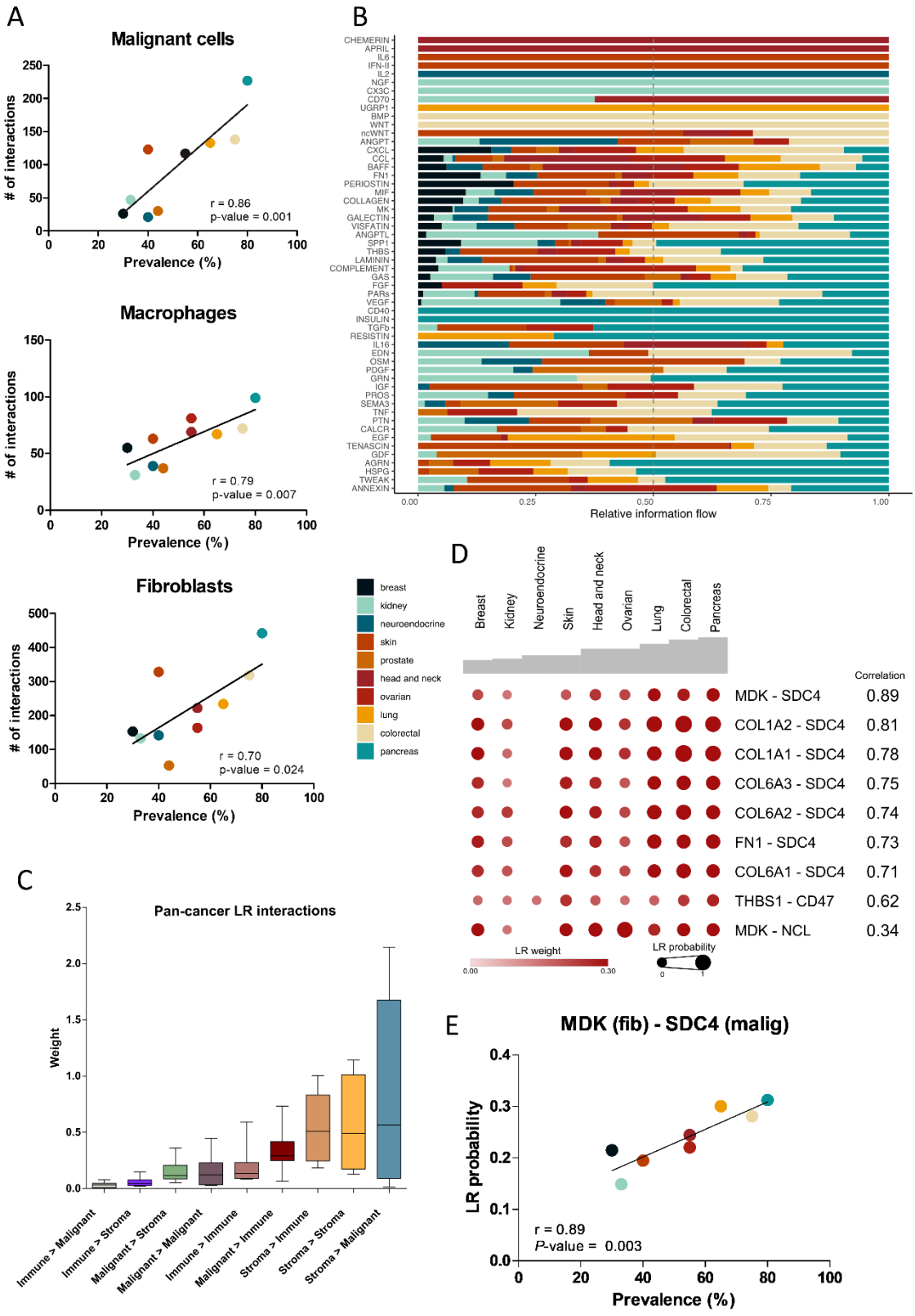

Figure 2. Tumor microenvironment cell-cell communication patterns correlate with cachexia prevalence in human cancers A) Scatterplot showing the Pearson correlation of the proportion of ligand-receptor interactions and cachexia prevalence. **B)** Stacked bar graph demonstrating the communication pathways enriched in each tumor type according to the ligand-receptor interactions. **C)** Box plot demonstrating the weight of ligand and receptors (LR) interactions between tumor microenvironment cells

considering 10 cancer types. “Immune” comprises macrophages, T cells, B cells, and dendritic cells. “Stroma” comprises fibroblasts and endothelial cells. **D)** Heat-scatter plot presenting the proportion of ligand-receptor (LR) interactions weights. The values represent the Pearson correlation of LR weights and cachexia prevalence (upper bar). **E)** Scatterplot showing the Pearson correlation of the interaction probability of MDK (expressed by fibroblast) and its receptor SDC4 (expressed by malignant cells) with cachexia prevalence among human cancer types.

Final Remarks

We characterized the secretome profile and the communications prometed by the secretome in TME single cells using a pan-cancer strategy. This approach allowed us to identify the specific communication patterns of the cell types correlating with cachexia prevalence. We found that the higher the number of upregulated secretome genes in malignant cells and fibroblasts, the higher the cachexia prevalence. Cell-cell communication analyses based on the secretome demonstrated that high cachexia prevalence correlates with increased interactions in fibroblasts, macrophages, and malignant cells. These interactions also indicate the essential role of fibroblast secretome in cancers with a high prevalence of cachexia, with pancreatic cancer impacting the highest number of cell-cell communication pathways. Among the interaction probabilities, *MDK* expressed by fibroblasts and its receptors *SDC4*, expressed by malignant cells, highly correlate (0.89; p=0.003) with cachexia prevalence. Interestingly, the communication of *MDK-SDC4* were recently demonstrated as players in TME immunosuppression and lower survival in colorectal cancer patients [8]. In conclusion, we characterized the secretome expression profile and communication patterns in a single-cell resolution according to the prevalence of cachexia in 10 tumor types. These findings pave the way for future studies to explore the described targeted therapies in cancer cachexia patients and animal models of the disease.

4. Referências

1. Gavish A, Tyler M, Greenwald AC, et al. Hallmarks of transcriptional intratumour heterogeneity across a thousand tumours. *Nature*. Published online May 31, 2023:1-9. doi:10.1038/s41586-023-06130-4

2. Satija R, Farrell JA, Gennert D, Schier AF, Regev A. Spatial reconstruction of single-cell gene expression data. *Nat Biotechnol*. 2015;33(5):495-502. doi:10.1038/nbt.3192

3. Stuart T, Butler A, Hoffman P, et al. Comprehensive Integration of Single-Cell Data. *Cell*. 2019;177(7):1888-1902.e21. doi:10.1016/j.cell.2019.05.031

4. Jin S, Guerrero-Juarez CF, Zhang L, et al. Inference and analysis of cell-cell communication using CellChat. *Nat Commun*. 2021;12(1):1088. doi:10.1038/s41467-021-21246-9

5. Poisson J, Martinez-Tapia C, Heitz D, et al. Prevalence and prognostic impact of cachexia among older patients with cancer: a nationwide cross-sectional survey (NutriAgeCancer). *J Cachexia Sarcopenia Muscle*. 2021;12(6):1477-1488. doi:10.1002/jcsm.12776

6. Brinksma A, Huizinga G, Sulkers E, Kamps W, Roodbol P, Tissing W. Malnutrition in childhood cancer patients: A review on its prevalence and possible causes. *Crit Rev Oncol Hematol*. 2012;83(2):249-275. doi:10.1016/j.critrevonc.2011.12.003

7. Freire PP, Fernandez GJ, Moraes D de, et al. The expression landscape of cachexia-inducing factors in human cancers. *J Cachexia Sarcopenia Muscle*. 2020;11(4):947-961. doi:10.1002/jcsm.12565

8. Hashimoto M, Kojima Y, Sakamoto T, et al. Spatial and single-cell colocalisation analysis reveals MDK-mediated immunosuppressive environment with regulatory T cells in colorectal carcinogenesis. *eBioMedicine*. 2024;103:105102. doi:10.1016/j.ebiom.2024.105102

5. Anexos

Supplementary table 1. Samples and datasets included in the study.

Accession number	Sample	Cancer
GSE144236	P1	SCC Skin
	P2	SCC Skin
	P3	SCC Skin
	P4	SCC Skin
	P5	SCC Skin
	P6	SCC Skin
	P7	SCC Skin
	P8	SCC Skin
	P9	SCC Skin
GSE141445	1	Prostate Cancer
	2	Prostate Cancer
	3	Prostate Cancer
	4	Prostate Cancer
	5	Prostate Cancer
	6	Prostate Cancer
	7	Prostate Cancer
	8	Prostate Cancer
	10	Prostate Cancer
	11	Prostate Cancer
	12	Prostate Cancer
	13	Prostate Cancer
EGAS00001002325	4602STDY6930850	RCC
	4602STDY6930851	RCC
	4602STDY6930854	RCC
	4602STDY6930855	RCC
	4602STDY6949182	RCC
	4602STDY6949183	RCC
	4602STDY6976422	RCC
	4602STDY6976423	RCC
	4602STDY6976424	RCC
	4602STDY6976425	RCC
	4602STDY7018624	RCC
	4602STDY7018625	RCC
	4602STDY7018626	RCC
	4602STDY7018627	RCC
phs002065.v1.p1	P76	RCC
	P90	RCC
https://dx.doi.org/10.17632/nc9bc8dn4m.1	Patient1	RCC

	Patient2	RCC
	Patient3	RCC
	Patient4	RCC
	Patient5	RCC
	Patient6	RCC
	Patient7	RCC
	Patient8	RCC
GSE159115	SI_18854	RCC
	SI_18855	RCC
	SI_19703	RCC
	SI_22368	RCC
	SI_22604	RCC
	SI_23459	RCC
	SI_23843	RCC
GSE150430	P01	NPC
	P02	NPC
	P03	NPC
	P04	NPC
	P05	NPC
	P06	NPC
	P07	NPC
	P08	NPC
	P09	NPC
	P10	NPC
	P11	NPC
	P12	NPC
	P14	NPC
	P15	NPC
EGAS00001004388	NB01	NB
	NB03	NB
	NB04	NB
	NB06	NB
	NB07	NB
	NB08	NB
	NB09	NB
	NB10	NB
	NB11	NB
	NB12	NB
EGAD00001008345	PD42184	NB
	PD42752-1	NB
	PD42752-2	NB
	PD43255	NB
	PD46693	NB
GSE137804	Tumor_10	NB
	Tumor_162	NB

	Tumor_19	NB
	Tumor_200	NB
	Tumor_230	NB
	Tumor_27	NB
	Tumor_34	NB
	Tumor_40	NB
	Tumor_44	NB
	Tumor_69	NB
	Tumor_71	NB
	Tumor_75	NB
	Tumor_92	NB
GSE154778	P01	PDAC
	P02	PDAC
	P03	PDAC
	P04	PDAC
	P05	PDAC
	P06	PDAC
	P07	PDAC
	P08	PDAC
	P09	PDAC
	P10	PDAC
CRA001160	T11	PDAC
	T13	PDAC
	T14	PDAC
	T15	PDAC
	T16	PDAC
	T17	PDAC
	T19	PDAC
	T2	PDAC
	T20	PDAC
	T21	PDAC
	T22	PDAC
	T3	PDAC
	T6	PDAC
	T7	PDAC
	T8	PDAC
	T9	PDAC
GSE155698	PDAC_TISSUE_1	PDAC
	PDAC_TISSUE_10	PDAC
	PDAC_TISSUE_11A	PDAC
	PDAC_TISSUE_11B	PDAC
	PDAC_TISSUE_12	PDAC
	PDAC_TISSUE_13	PDAC
	PDAC_TISSUE_15	PDAC
	PDAC_TISSUE_2	PDAC

	PDAC_TISSUE_3	PDAC
	PDAC_TISSUE_4	PDAC
	PDAC_TISSUE_5	PDAC
	PDAC_TISSUE_6	PDAC
	PDAC_TISSUE_7	PDAC
	PDAC_TISSUE_8	PDAC
	PDAC_TISSUE_9	PDAC
	PDAC_TISSUE_16	PDAC
EGAS00001002185, EGAS00001001900, and EGAS00001003845	SF10022	GBM
	SF10127	GBM
	SF11979sn	GBM
	SF12090	GBM
	SF12264	GBM
	SF4297	GBM
	SF4400	GBM
	SF6996	GBM
	SF9259R	GBM
	SF9259S	GBM
GSE148673	TNBC1	BRCA
	TNBC2	BRCA
	TNBC3	BRCA
	TNBC4	BRCA
	TNBC5	BRCA
GSE161529	ER_positive_0001	BRCA
	ER_positive_0025	BRCA
	ER_positive_0029_7C	BRCA
	ER_positive_0029_9C	BRCA
	ER_positive_0032	BRCA
	ER_positive_0040	BRCA
	ER_positive_0043	BRCA
	ER_positive_0056	BRCA
	ER_positive_0064	BRCA
	ER_positive_0114	BRCA
	ER_positive_0125	BRCA
	ER_positive_0151	BRCA
	ER_positive_0163	BRCA
	ER_positive_0167	BRCA
	ER_positive_0173	BRCA
	ER_positive_0360	BRCA
	HER2_0069	BRCA
	HER2_0161	BRCA
	HER2_0176	BRCA
	HER2_0308	BRCA
	HER2_0331	BRCA
	HER2_0337	BRCA

	PR_positive_0319	BRCA
	Triple_negative_0106	BRCA
	Triple_negative_0114	BRCA
	Triple_negative_0126	BRCA
	Triple_negative_0135	BRCA
	Triple_negative_BRCA1_0131	BRCA
	Triple_negative_BRCA1_0177	BRCA
	Triple_negative_BRCA1_0554	BRCA
	Triple_negative_BRCA1_4031	BRCA
E-MTAB-8107	42	BRCA
	43	BRCA
	47	BRCA
	49	BRCA
	51	BRCA
	53	BRCA
	54	BRCA
E-MTAB-8107	BT1306	OV
	BT1307	OV
	scrSOL001	OV
	scrSOL003	OV
	scrSOL004	OV
GSE131907	P0034	LUAD
	P0031	LUAD
	P1028	LUAD
	P0019	LUAD
	P0030	LUAD
	P0028	LUAD
	P0006	LUAD
	P1049	LUAD
	P0008	LUAD
	P1058	LUAD
	P0025	LUAD
	P0020	LUAD
	P0018	LUAD
	P1006	LUAD
GSE123904	RU653	LUAD
	RU661	LUAD
	RU675Tum	LUAD
	RU676	LUAD
	RU680	LUAD
	RU682Tum	LUAD
	RU684Tum	LUAD
HRA000154	SSN05	LUAD
	SSN09	LUAD
	SSN10	LUAD

	SSN11	LUAD
	SSN12	LUAD
	SSN19	LUAD
	SSN21	LUAD
	SSN22	LUAD
	SSN24	LUAD
	SSN25	LUAD
	SSN27	LUAD
	SSN28	LUAD
	SSN29	LUAD
	SSN30	LUAD
	SSN31	LUAD
	SSN33	LUAD
E-MTAB-6149	BT1290 (LC3)	LUAD
	BT1291 (LC3)	LUAD
	BT1292 (LC3)	LUAD
	BT1295 (LC4)	LUAD
	BT1296 (LC4)	LUAD
	BT1297 (LC4)	LUAD
	scrBT1430 (LC6)	LUAD
	scrBT1431 (LC6)	LUAD
	scrBT1432 (LC6)	LUAD
PRJNA694128	27522_Primary	Multiple myeloma
	37692_Primary	Multiple myeloma
	47491_Primary	Multiple myeloma
	56203_Primary	Multiple myeloma
	58408_Primary	Multiple myeloma
	59114_Primary	Multiple myeloma
	60359_Primary	Multiple myeloma
	77570_Primary	Multiple myeloma
	81012_Primary	Multiple myeloma
	83942_Primary	Multiple myeloma
GSE141445 e HRA000312	SMC01-T	Colorectal cancer
	SMC02-T	Colorectal cancer
	SMC04-T	Colorectal cancer
	SMC07-T	Colorectal cancer
	SMC08-T	Colorectal cancer
	SMC09-T	Colorectal cancer
	SMC11-T	Colorectal cancer
	SMC14-T	Colorectal cancer
	SMC15-T	Colorectal cancer
	SMC16-T	Colorectal cancer
	SMC18-T	Colorectal cancer
	SMC20-T	Colorectal cancer
	SMC21-T	Colorectal cancer

	SMC23-T	Colorectal cancer
	SMC25-T	Colorectal cancer

BRCA: breast cancer; LUAD: lung adenocarcinoma; OV: ovarian cancer; GBM: glioblastoma; PDAC: pancreatic ductal adenocarcinoma; NB: neuroblastoma; NPC: nasopharyngeal cancer; RCC: renal cell carcinoma; SCC: squamous cell carcinoma.

6. Outras atividades realizadas durante o período da bolsa

Apresentação e participação em eventos científicos:

- Brunch da Internacionalização da Pós-graduação 2024. UNESP. Palestrante.
- 1º Encontro do Programa de Pós-Doutorado da Unesp. Ouvinte.

Prêmio

- Prêmio UNESP de Teses 6ª edição.

Bolsa de IC concedida/solicitada:

- Concedida: Mateus Alves Diniz. Reposicionamento de drogas para o tratamento de precisão de adenocarcinomas pulmonares utilizando a reversão do perfil transcricional de células neoplásicas únicas. Bolsa PIBIC Reitoria.

Atividades de docência:

- Special Topics: Muscle metabolism in health condition and older people: from bench to bedside. PPG Cirurgia e Medicina Translacional. 15 horas (1 crédito).

Participação de bancas:

- Rafaela Alves Ribeiro. Identificação de genes inversamente regulados por aminoácidos e IGF1 em células musculares do pacu (*Piaractus mesopotamicus*) e gilthead sea bream (*Sparus aurata*). Qualificação de Mestrado.
- Vanessa das Graças Pereira de Souza. Caracterização do transcritoma codificador da metástase cerebral de câncer de pulmão. Defesa de Doutorado.
- Raphaela Neto Pereira. Diversidade do gene *KIR3DL2* em diferentes populações e continentes. Qualificação de Doutorado.

Publicações:

- LOPES, LETÍCIA OLIVEIRA; **CURY, SARAH SANTILONI**; DE MORAES, DIOGO; OLIVEIRA, JAKELINE SANTOS; DE OLIVEIRA, GRASIELI; CABRAL-MARQUES, OTAVIO; FERNANDEZ, GEYSSON JAVIER; HIRATA, MARIO HIROYUKI; WANG, DA-ZHI; DAL-PAI-SILVA, MAELI; CARVALHO, ROBSON FRANCISCO; FREIRE, PAULA PACCIELLI. The Impact of miR-155-5p on Myotube Differentiation: Elucidating Molecular Targets in Skeletal Muscle Disorders. INTERNATIONAL JOURNAL OF MOLECULAR SCIENCES, v. 25, p. 1777, 2024. doi: 10.3390/ijms25031777.